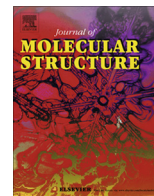




Contents lists available at ScienceDirect

Journal of Molecular Structure

journal homepage: www.elsevier.com/locate/molstruc

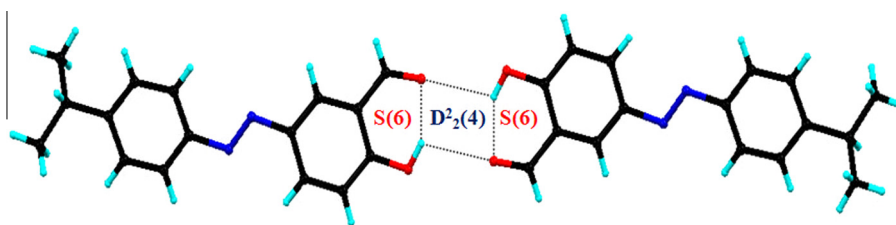
A novel azo-aldehyde and its Ni(II) chelate; synthesis, characterization, crystal structure and computational studies of 2-hydroxy-5-*((E)*-[4-(propan-2-yl)phenyl]diazenyl)benzaldehyde

Tuğba Eren^a, Muhammet Kose^a, Koray Sayin^b, Vickie McKee^c, Mukerrem Kurtoglu^{a,*}^a Department of Chemistry, Kahramanmaraş Sütçü İmam University, Kahramanmaraş 46050, Turkey^b Department of Chemistry, Cumhuriyet University, Sivas 58140, Turkey^c Department of Chemistry, Loughborough University, Leicestershire LE11 3TU, UK

HIGHLIGHTS

- A novel azo-salicylaldehyde and its Ni(II) chelate were synthesized and characterized by analytical and spectroscopic studies.
- The X-ray structure of the azo-salicylaldehyde was determined.
- The OH...O intra-intermolecular hydrogen bondings and π - π interactions stabilize the crystal structure.
- Optimized structures of the three possible tautomers were obtained using B3LYP method.

GRAPHICAL ABSTRACT



ARTICLE INFO

Article history:

Received 27 December 2013

Received in revised form 14 February 2014

Accepted 27 February 2014

Available online 6 March 2014

Keywords:

Azo-aldehyde

Ni(II) chelate

X-ray diffraction

Solvent effect

 π - π Interactions

Quantum chemical studies

ABSTRACT

A novel azo-salicylaldehyde, 2-hydroxy-5-*((E)*-[4-(propan-2-yl)phenyl]diazenyl) benzaldehyde and its Ni(II) chelate were obtained and characterized by analytical and spectral techniques. Molecular structure of the azo chromophore containing azo-aldehyde was determined by single crystal X-ray crystallography. X-ray data show that the compound crystallizes in the orthorhombic, *Pbca* space group with unit cell parameters $a = 11.2706(9)$, $b = 8.3993(7)$, $c = 28.667(2)$ Å, $V = 2713.7(4)$ Å³ and $Z = 8$. There is a strong phenol-aldehyde (OH...O) hydrogen bond forming a S(6) hydrogen bonding motif in the structure. There is also a weaker inter-molecular phenol-aldehyde (OH...O) hydrogen bonding resulting in a dimeric structure and generating a D₂²(4) hydrogen bonding motif. Hydrogen bonded dimers are linked by π - π interactions within the structure. The azo-aldehyde ligand behaved as bidentate, coordinating through the nitrogen atom of the azomethine group and or oxygen atom of phenolic hydroxyl group. Additionally, optimized structures of the three possible tautomers of the compound were obtained using B3LYP method with 6-311++G(d,p), 6-31G and 3-21G basis sets in the gas phase. B3LYP/6-311++G(d,p) level is found to be the best level for calculation. The electronic spectra of the compounds in the 200–800 nm range were obtained in three organic solvents.

© 2014 Elsevier B.V. All rights reserved.

1. Introduction

The interest in studies of compounds derived from salicylaldehyde and its derivatives is increasing day by day [1]. Condensation

reactions of salicylaldehyde and its derivatives with various primary aromatic or aliphatic mono-, di-, tri- or polyamines result in compounds containing azomethine bond (—C=N—) known as Schiff bases [2,3]. These compounds form coordination compounds with several metal ions [4]. There are numerous papers published on salicylaldehyde and its derivatives regarding their fluorescent and use as colorimetric sensors [5,6], antitumor activity [7], and DNA cleavage activity [8].

* Corresponding author. Tel.: +90 344 280 1450; fax: +90 344 280 1352.

E-mail addresses: mkurtoglu@ksu.edu.tr, kurtoglu01@gmail.com (M. Kurtoglu).

Azo containing compounds are of interest due to their properties including the dyeing of textiles [9], optical switching, non-linear optical properties [10], and the preparation of photoactive materials [11]. Synthesis of azo containing dyes dates back to the second half of the 20th century, since then azo dyes have attracted a great deal of attention and found many uses in textile industry as well as material sciences [12]. Azo compounds are reported to be involved in a number of biological systems such as inhibition of DNA, RNA, and protein synthesis, carcinogenesis, and nitrogen fixation [13,14]. In addition, azo compounds and their metal chelates have shown a good anti-bacterial activity [15,16]. These compounds are also used in analytical chemistry as indicators in pH, redox, or complexometric titration [17,18].

There is a close relationship between the physico-chemical properties of azo dyes and tautomerism [19]. Due to the affect of tautomerism of azo dyes on different technical properties and dyeing abilities, theoretical and experimental studies of tautomers have attracted much attention [20].

Because of the importance of azo-salicylaldehyde derivatives and our continuing interest in synthesis of azo and azomethine compounds, a novel azo-aldehyde compound, 2-hydroxy-5-((*E*)-[4-(propan-2-yl)phenyl]diazanyl)benzaldehyde, ¹pr-salH (Fig. 1) and its Ni(II) complex were prepared and characterized by spectroscopic and analytic methods. Molecular structure of the title compound was determined by single crystal X-ray diffraction studies. The properties of the azo-aldehyde ¹pr-salH were determined computationally by DFT method at the B3LYP/6-31G(d,p) level of theory. Furthermore, the solvatochromic behavior of the prepared azo compounds in various solvents was evaluated.

2. Experimental

2.1. Reagents

All reagents and solvents were purchased from chemical companies and used without further purification unless otherwise noted. The UV–Vis spectra were taken in spectrophotometric grade solvents.

2.2. Physical measurements

NMR spectra were performed using a Bruker Advance 400 MHz. Spectrometer. Mass spectra were recorded on a Thermo Fisher Exactive + Triversa Nanomate mass spectrometer. The infrared spectra were obtained using a Perkin Elmer spectrum 100 FTIR spectrophotometer. Carbon, hydrogen and nitrogen analyses were performed with a model CE-440 elemental analyzer. Single crystals suitable for X-ray diffraction study were obtained from CHCl₃-EtOH solution by slow evaporation at room temperature. Data collection for X-ray crystallography was completed using a Bruker APEX2 CCD diffractometer and data reduction was performed using Bruker SAINT [21]. SHELXTL was used to solve and refine the structures [22]. The UV–Vis spectra were measured with a T80 + UV–Vis. Spectrometer PG Instruments Ltd.

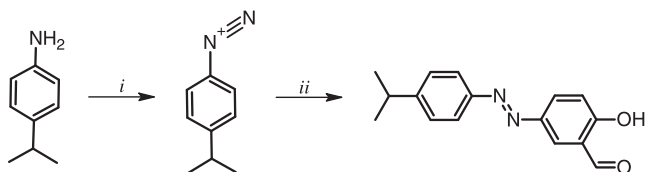


Fig. 1. Synthesis of 2-hydroxy-5-((*E*)-[4-(propan-2-yl)phenyl]diazanyl)benzaldehyde (¹pr-salH). i: NaNO₂/HCl, 273–278 K; ii: salicylaldehyde.

2.3. Crystallography

A single crystal of dimensions 0.46 × 0.45 × 0.15 mm³ was chosen for the diffraction experiment. Data were collected at 150(2)K on a Bruker ApexII CCD diffractometer using Mo K α radiation ($\lambda = 0.71073$ Å). The structure was solved by direct methods and refined on F^2 using all the reflections [22]. All the non-hydrogen atoms were refined using anisotropic atomic displacement parameters and hydrogen atoms bonded to carbon atoms were inserted at calculated positions using a riding model. Hydrogen atom bonded to oxygen atom (O1) was located from difference maps and refined with temperature factor riding on the carrier atom. Details of the crystal data and refinement are given in Table 1. Hydrogen bond parameters are listed in Table 2, bond lengths and angles are given in Tables 1S and 2S.

2.4. Computational method

All calculations were made by using Gaussian 09 [23,24]. Density functional theory (DFT) methods [25,26], containing the Becke three parameters hybrid exchange and the Lee–Yang–Parr correlation hybrid functional (B3LYP) [27–29] were used in geometry optimization. In the first step, tautomer (1) was fully optimized by using B3LYP method with 6-311++G(d,p), 6-31G and 3-21G basis sets in gas phase. The best level was found to be B3LYP/6-311++G(d,p). In the second step, tautomers (2) and (3) were fully optimized by using the best level in gas phase. 6-311++G(d,p) is a popular high angular momentum basis set which adds p functions to hydrogen and d functions on heavy atoms. The transition state (TS) method was used to search for the transition states of all reaction paths [30,31]. The analyses of vibrational frequencies indicated that optimized structures of transition states were at stationary points corresponding to local minima with imaginary frequencies which are equal to 1.

2.5. Synthesis of 2-hydroxy-5-((*E*)-[4-(propan-2-yl)phenyl]diazanyl)benzaldehyde, ¹pr-salH

The title compound, (¹pr-salH), was synthesized following standard protocols [32], using *p*-isopropylaniline and salicylaldehyde as starting materials: A mixture of 4-isopropylaniline (1.35 g, 10 mmol), water (50 mL) and concentrated hydrochloric acid (2.5 mL, 30 mmol) was stirred until a clear solution was obtained.

Table 1
Crystallographic data for the ¹pr-salH compound.

Identification code	¹ pr-salH
Empirical formula	C ₁₆ H ₁₆ N ₂ O ₂
Formula weight	268.31
Crystal size (mm ³)	0.46 × 0.45 × 0.15
Crystal color	Orange
Crystal system	Orthorhombic
Space group	Pbca
<i>Unit cell</i>	
<i>a</i> (Å)	11.2706(9)
<i>b</i> (Å)	8.3993(7)
<i>c</i> (Å)	28.667(2)
Volume (Å ³)	2713.7(4)
<i>Z</i>	8
Abs. coeff. (mm ⁻¹)	0.088
Refl. collected	25992
Completeness to $\theta = 28.02^\circ$	99.9%
Ind. Refl. [<i>R</i> _{int}]	3377 [0.0404]
<i>R</i> ₁ , <i>wR</i> ₂ [<i>I</i> > 2 σ (<i>I</i>)]	0.0394, 0.1011
<i>R</i> ₁ , <i>wR</i> ₂ (all data)	0.0550, 0.1093
CCDC number	947938

Table 2
Hydrogen bonds for ⁱpr-salH [Å and °].

D—H...A	d(D—H)	d(H...A)	d(D...A)	<(DHA)
O(1)—H(1)...O(2)#1	0.88	2.55	2.9819(13)	111.2
C(16)—H(16)...O(1)#2	0.93	2.57	3.3056(16)	136.8
O(1)—H(1)...O(2)	0.88	1.86	2.6537(13)	149.9

Symmetry transformations used to generate equivalent atoms:
#1 $-x, -y, -z + 1$; #2 $x + 1/2, -y + 1/2, -z + 1$.

This solution was cooled to 273–278 K and a solution of sodium nitrite (0.96 g, 11.29 mmol) in water (3 mL) was added dropwise while the temperature was maintained below 278 K. The resulting mixture was stirred for 30 min in an ice bath. An *o*-hydroxybenzaldehyde (1.22 g, 10 mmol) solution (pH 9–10) was added gradually to the solution of cooled 4-isopropylbenzenediazonium chloride, prepared as described above, and the resulting mixture was stirred at 273–278 K for 60 min. The dark yellow product was filtered off, washed with MeOH and dried in air. Crystals of 2-hydroxy-5-[(*E*)-[4-(propan-2-yl)phenyl]diazonyl]benzaldehyde were obtained from slow evaporation of an EtOH-CHCl₃ mixture.

Yield, 2.24 g, 83%, m.p. 368–369 K. Elemental analyses for C₁₆H₁₆N₂O₂ (F.W. 268.12 g/mol): Calcd. (%): C, 71.61; H, 6.01; N, 10.45. Found (%): C, 71.39; H, 5.69; N, 10.33. IR (KBr, cm⁻¹): 3435 (—OH stretching), 3050 (aromatic), 2958–2866 (C—H stretching of methyl), 1654 (C=O stretching), 1577 (—N=N—). ¹H NMR (CDCl₃ as solvent, γ in ppm): 1.34 (*d*, 6H, CH₃), 2.99 (*s* (septet), 1H, CH), 6.93 (*d*, 1H, CH (aromatic)), 7.39 (*d*, 2H, CH (aromatic)), 7.94 (*d*, 2H, CH (aromatic)), 8.19 (*d*, 1H, CH (aromatic)), 8.21 (*s*, 1H, CH (aromatic)), 10.28 (*s*, 1H, HC=O), 11.33(*s*, 1H, OH). ¹³C NMR: 23.86 (C1, C3), 34.17 (C2), 118.52–152.52 (aromatic C), 163.53 (C—OH), 196.62 (C=O). ESI mass (*m/z*): 269(40%) [M + H]⁺, 323(100%) [M + Na + CH₃OH]⁺, 537(75%) [2 M + H]⁺, 553 (75%) [2 M + ·OH]⁺.

2.6. Synthesis of [Ni(ⁱpr-sal)₂]·5H₂O

To a hot solution (0.2 g, 0.75 mmol) of 2-hydroxy-5-[(*E*)-[4-(propan-2-yl)phenyl]diazonyl]benzaldehyde in (35 mL) MeOH, a hot solution of Ni(CH₃COO)₂·4H₂O (0.09 g, 0.373 mmol, in 25 mL MeOH) was added slowly. The resulting mixture was stirred and refluxed on a hot plate for 3 h, and then concentrated to half its initial volume. After cooling for the mixtures overnight, the solid product is precipitated and separated, washed with cold MeOH and Et₂O and dried in air.

Yield, 0.65 g, 73%, m.p. 537–538 K. Elemental analyses for C₃₂H₄₀N₄NiO₉ (F.W. 683.37 g/mol): Calcd. (%): C, 56.24; H, 5.90; N, 8.20. Found (%): C, 55.57; H, 5.985; N, 8.48. IR (KBr, cm⁻¹): 3559 (—OH stretching), 3050 (C—H aromatic), 2961–2866 (C—H aliphatic), 1626 (C=O stretching), 1464 (—N=N—), 501 (Ni—O), 464 (Ni—O).

3. Result and discussion

3.1. Synthesis and spectroscopic studies

The azo-aldehyde (ⁱpr-salH) was synthesized from the solution of 4-isopropylaniline diazonium salt and salicylaldehyde using the classical reaction for the preparation of azo compounds (Fig. 1). The Ni(II) complex [Ni(ⁱpr-sal)₂]·5H₂O was prepared by the reaction of two equivalents of ⁱpr-salH and one equivalent of Ni(CH₃COO)₂·4H₂O in MeOH (Fig. 2). The compounds were characterized using microanalyses and spectroscopic techniques. The microanalytical results are in good agreement with formulation. Both the ligand and its Ni(II) complex are stable at room temperature in the solid

state without decomposition. The ligand is soluble in a wide range of common organic solvents such as methanol, acetonitrile, chloroform, dichloromethane, dimethylformamide and dimethylsulfoxide, but is insoluble in water.

The ¹H and ¹³C NMR spectra of the azo-aldehyde ligand were recorded in CDCl₃, and the spectral data are given in the experimental section. ¹H and ¹³C NMR spectra are displayed in Figs. 1S and 2S respectively. The ¹H NMR spectrum displays a doublet at δ 1.34 ppm corresponding to protons of two identical methyl groups (C—CH₃), a septet at δ 2.99 ppm assigned to the proton of the isopropyl carbon atom (—CH—). The signal assigned to the carbonyl proton was seen at δ 10.28 ppm and one broad signal at δ 11.33 ppm was assigned to phenolic protons (OH). All aromatic protons were seen in the range of δ 6.93–8.21 ppm (Fig. 1S).

The ¹³C NMR spectrum of the azo-aldehyde exhibited the signals due to the presence of aromatic and aliphatic carbons. The presence of carbonyl group is evident from the characteristic signal at the farthest downfield ~196.62 ppm corresponding to the carbon of —CHO group (C16) [33]. The peak at δ 163.53 ppm was assigned to the aromatic carbon linked hydroxyl group (C13). The aliphatic region of the ¹³C NMR spectrum of ⁱpr-salH showed two peaks as seen in Fig. 2S. The medium intense peak CH₃ (23.86 ppm, (C1, C3), was conveniently assigned to the methyl carbon of the isopropyl group. The peak —CH— (34.17 ppm, (C2) is due to tertiary carbon according to the chemical shift. In the aromatic region of the ¹³C NMR spectrum of compound ⁱpr-salH, the peaks at δ 118.52–152.52 ppm were assigned to the aromatic carbons. The peaks were then tentatively assigned by matching the observed and calculated chemical shifts. The spectroscopic data obtained in this work agree well with the previous work [33].

In the infrared spectrum of the azo-aldehyde (Fig. 3S), a broad band at 3435 cm⁻¹ is attributed to intramolecular hydrogen bonded phenolic —OH group. The spectrum of the compound showed an intense carbonyl band (—C=O) at 1654 cm⁻¹, which corresponds to a highly conjugated system [34]. The carbonyl group produces a strong signal in the infrared spectrum, generally

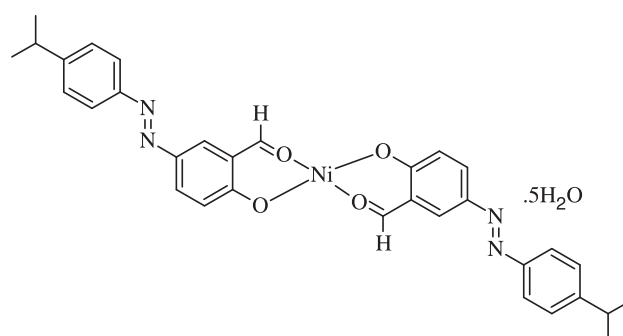


Fig. 2. The proposed structure of Ni(II) chelate of ⁱpr-salH azo-aldehyde.

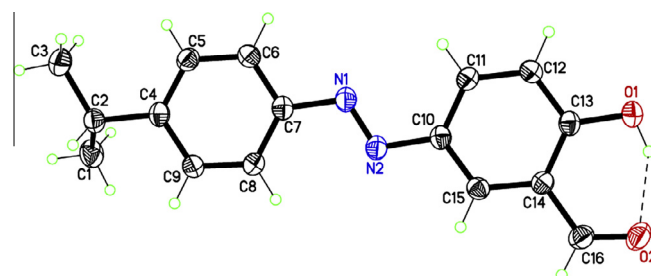


Fig. 3. Crystal structure of ⁱpr-salH with atom labeling (thermal ellipsoid 50% probability), hydrogen bonding is shown as dashed lines.

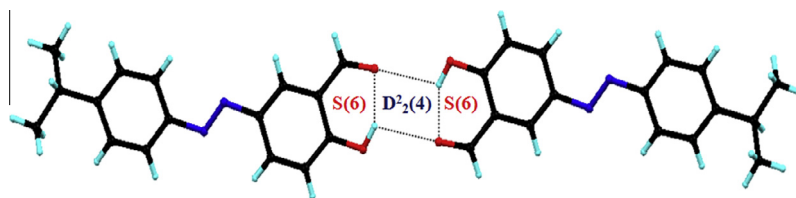


Fig. 4. Hydrogen bonded dimers, hydrogen bonds are shown as dash lines.

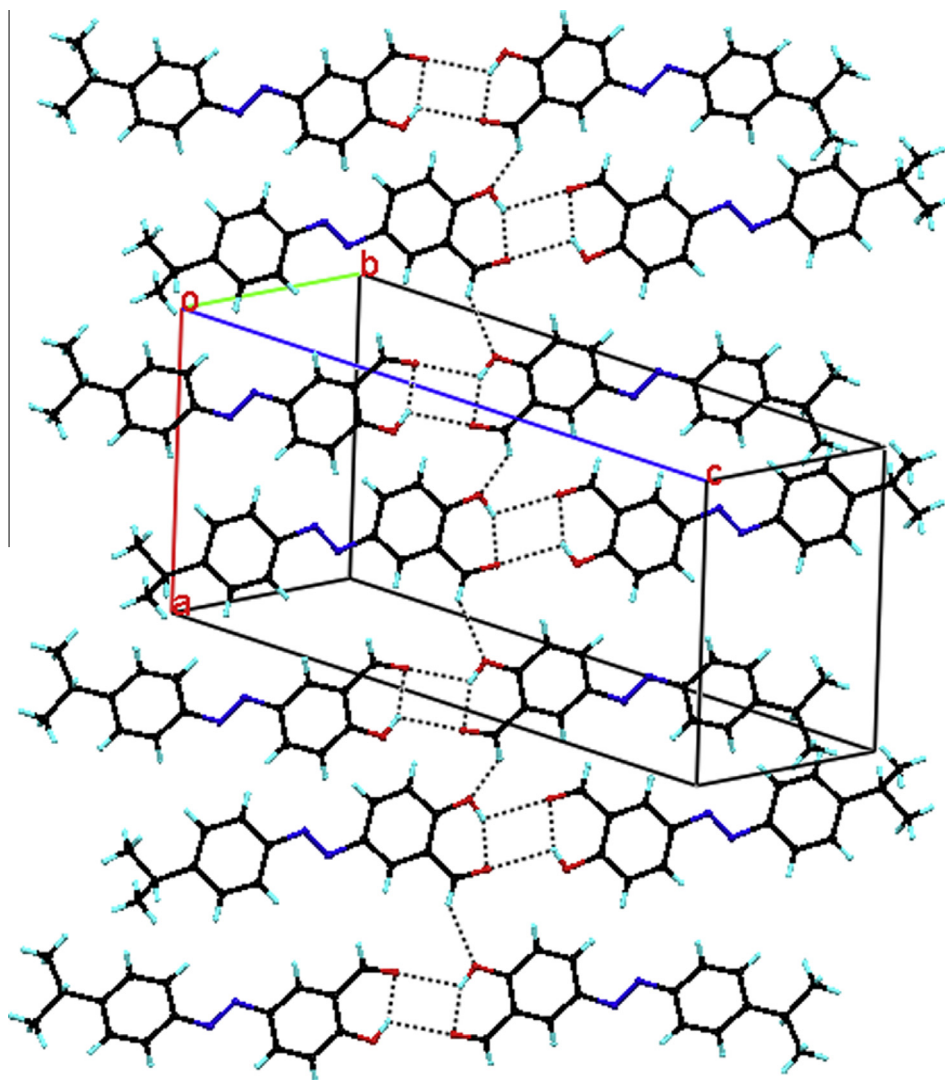


Fig. 5. Hydrogen bonding network in crystal packing, hydrogen bonding is shown as dashed lines.

around 1715 or 1695 cm^{-1} . However, a conjugated carbonyl will produce a signal at a lower wavenumber as a result of electron delocalization *via* resonance effects. Aldehydes generally exhibit one or two signals (C–H stretching) between 2700 and 2850 cm^{-1} . Bands at 2958 – 2866 cm^{-1} are assigned to asymmetric and symmetric stretching vibrations of isopropyl group, respectively. The azo-aldehyde compound, ⁱpr-salH shows a band at 1481 cm^{-1} could be assigned to the –N=N– azo chromophore group. The azo-aldehyde showed a band at 1382 cm^{-1} for $\nu(\text{C}=\text{C})$ of aromatic rings. The band at about 1261 cm^{-1} is attributed to $\nu(\text{C}-\text{O})$ (phenolic) stretching in the compound ⁱpr-salH [35].

In the infrared spectrum of the Ni(II) complex (Fig. 4S), C=O stretching shifted to lower wavenumbers (1626 cm^{-1}) denoting

that the oxygen atom of the carbonyl group is coordinated to the metal(II) ion. The bonding of the metal ion to the ligand through phenolic and carbonyl oxygen atoms is further supported by the presence of new bands in the 501 and 464 cm^{-1} due to the $\nu(\text{M}-\text{O}_{\text{phenoxy}})$ and $\nu(\text{Ni}-\text{O}_{\text{carbonyl}})$ vibrations, respectively.

The ESI mass spectrum of the title ligand showed signals at m/z 269 (40%), 323(100%) and 537(75%) assigned to $[\text{M} + \text{H}]^+$, $[\text{M} + \text{Na} + \text{CH}_3\text{OH}]^+$ and $[2\text{M} + \text{H}]^+$, respectively.

3.2. X-ray structure of the ligand (ⁱpr-salH)

A perspective view of the ⁱpr-salH azo-aldehyde is shown in Fig. 3. The compound crystallizes in the non-centric orthorhombic *Pbca*

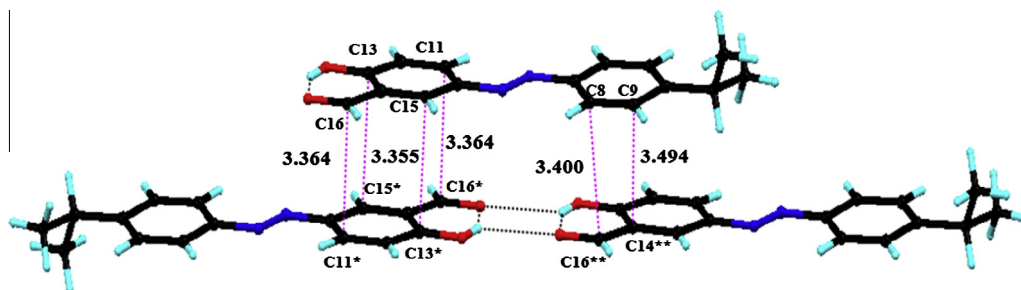


Fig. 6. $\pi \cdots \pi$ Interactions within the structure.

Table 3
Crystallographically characterized azo-salicylaldehydes.

Compound no.	R ₁	R ₂	R ₃	R ₄	Structure type	References
1	H	H	H	<i>i</i> -pr	Type 2	This work
2	H	H	H	Me	Type 2,3	[33,37,38]
3	H	H	H	Et	Type 1	[39]
4	H	H	H	Br	Type 3	[40]
5	H	H	H	Cl	Type 3	[41]
6	H	Cl	H	H	Type 2	[42]
7	OMe	H	H	H	Type 1	[43]
8	OMe	H	Br	H	Type 1	[44]
9	OMe	H	Cl	H	Type 1	[45]
10	OMe	F	H	H	Type 1	[46]
11	OMe	H	OMe	H	Type 1	[47]
12	OMe	H	H	<i>n</i> -butyl	Type 4	[48]

space group with unit cell parameters $a = 11.2706(9)$, $b = 8.3993(7)$, $c = 28.667(2)$ Å, $V = 2713.7(4)$ Å³ and $Z = 8$. All the bond lengths and angles are within the normal ranges. The aldehyde (C15=O2) and azo (N1=N2) distances are 1.2257(15) and 1.2574(14) Å respectively, which are in the range of C=O and N=N double bond character. Aromatic rings (C4–C9) and (C10–C15) adopt the *trans* configuration with regard to the azo double bond (–N=N–) with the torsion angle C(7)–N(1)–N(2)–C(10) of 179.62(9)°. In the structure, dihedral angles between two aromatic rings (C4–C9 and C10–C15) is 5.82(5)°.

There is a strong intra-molecular hydrogen bonding between phenolic O1–H1 with aldehyde oxygen (O1–O2 = 2.6535(14) Å) forming a S(6) hydrogen bonding motif. There is also a weaker inter-molecular O1–H1 \cdots O2* [–*x*, –*y*, –*z* + 1] hydrogen bonding joining two molecules together generating a D₂²(4) hydrogen bonding motif (Fig. 4). There are also CH(aldehydic) \cdots O interactions linking the molecules into hydrogen bonding network (Fig. 5 and Table 2) [36].

Hydrogen bonded dimers are linked by π – π interactions within the structure. There are two sets of π – π stacking; first, aldehyde-phenyl group (C11–C16) is stacked with the same section of neighbor molecule (symmetry operation: –*x*, 1 – *y*, 1 – *z*). C13–C15* is separated by 3.355 Å (Fig. 6); second, C8–C9 edge of one of molecule is stacked with C14–C16 edge of the adjacent molecule (symmetry operation: *x*, 1 + *y*, *z*).

It is informative to compare the structure of the title compound with related 5-arylo-azosalicylaldehyde derivatives reported in literature (Table 3). We have examined the structures of the 5-arylo-azosalicylaldehydes located in CCDC. Strong intramolecular hydrogen bond (OH \cdots O) was observed for almost all of the 5-ary-

lo-azosalicylaldehydes published. Additionally, each hydroxyl group can also make hydrogen bonds with the aldehyde oxygen of the neighboring molecule resulting in either chain or dimeric structure. Four different hydrogen bonding motifs, labeled type 1–4, appear in this series (Fig. 7 and Table 3).

The title compound (1-pr-salH) exhibits the dimeric structure (type 2). All of the 5-arylo-azosalicylaldehyde derivatives published show simple intramolecular hydrogen bonding. 4-Ethyl compound (3) shows the type 1 however the closely related 4-bromo (4) and 4-chloro (5) compounds adopt the chain structure (type 3). 4-Methyl compound (2) was initially published by two separate groups in monoclinic forms exhibiting dimeric structure (type 2), however the same compound was later reported as an orthorhombic form showing the chain structure (type 3). Both monoclinic and orthorhombic forms of 4-methyl compound (2) exhibit similar π – π stacking (phenyl–phenyl) interactions. Each polymorph was re-crystallised in different solvents (monoclinic form in DMSO, orthorhombic form in MeOH). The reason why the same compound shows two distinct crystal systems may be due to a small energy gap between these two forms. Related 2-chloro analogue (6) shows the dimeric structure (type 2).

Most of the 5-arylo substituted 3-metoxysalicylaldehyde derivatives (7–11) adopt the type 1 structure which only has an intramolecular hydrogen bonding (OH \cdots O). There is only one compound which shows no intramolecular hydrogen bond (OH \cdots O) but involves in intermolecular hydrogen bonding with neighboring molecules producing hydrogen bonded chain. This is rather unusual phenomenon for salicylaldehyde derivatives. The compound (12) shows no intramolecular hydrogen bond (OH \cdots O) but involves in intermolecular hydrogen bonding (OH \cdots O) with adjacent molecules forming hydrogen bonded chain (type 4).

3.3. Optimized structures of the azo aldehyde

Fig. 8 shows the optimized structures of three possible tautomers (1), (2) and (3). Calculated bond lengths and angles of tautomers (1–3) were given in Tables 1S and 2S, respectively.

Compared with experimental data and calculated bond lengths/angles of tautomer (1), it can be seen that B3LYP/6-311++G(d,p) level is the best level. As can be seen from Table 1S, the differences average between experimental and calculated bond lengths of tautomer (1) is 0.008 Å. According to the Table 2S, the differences average between experimental and calculated bond angles of tautomer (1) is 0.6°. These results show that there is a good agreement with experimental and optimized structure of tautomer (1). The structures of tautomers (2) and (3) were optimized with B3LYP/6-311++G(d,p).

3.4. The stability of tautomers

Some quantum chemical parameters such as total energy (E_{Total}) and Gibbs free energy (G°), were calculated to predict the stability of tautomers in gas phase and given in Table 4.

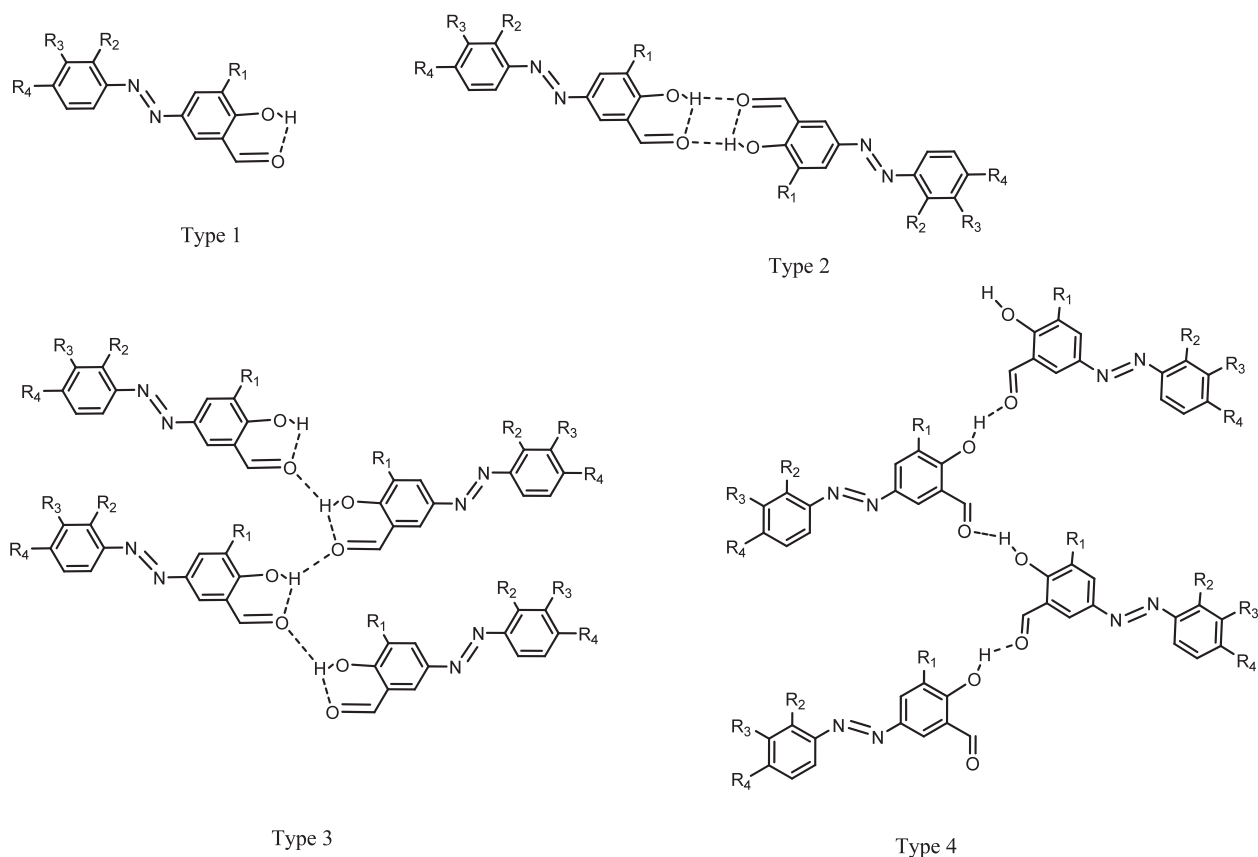


Fig. 7. Hydrogen bonding motifs reported for azo-salicylaldehydes.

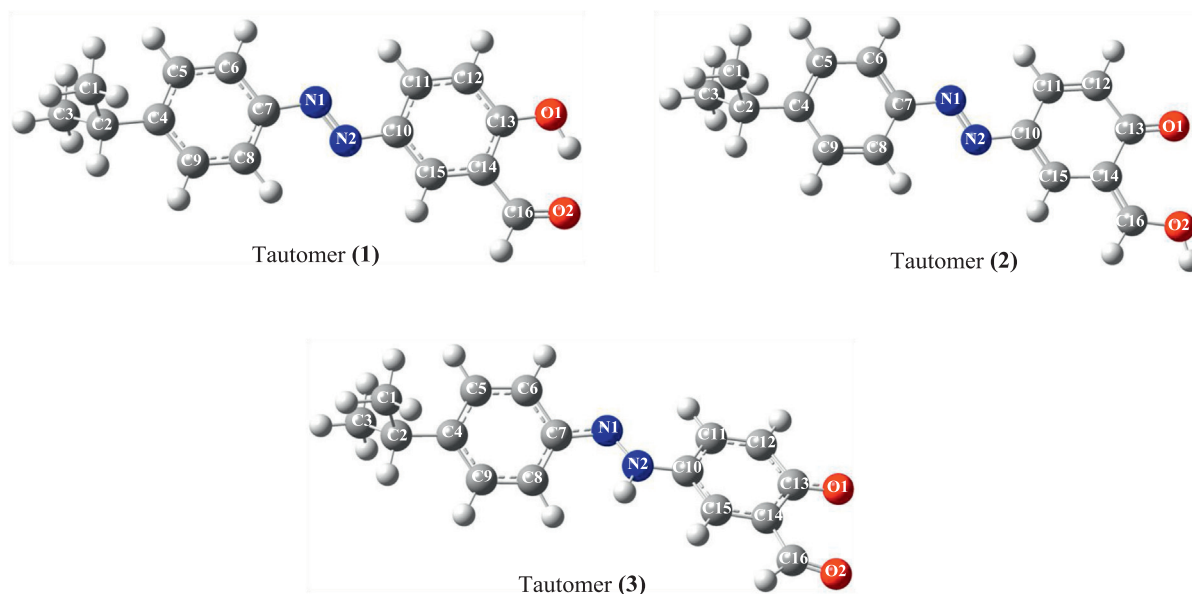


Fig. 8. Optimized structures of tautomers (1–3) with atom labeling.

$$E_{\text{Total}} = E_{\text{Thermal}} + E_{\text{Rotational}} + E_{\text{Vibrational}} + E_{\text{Electronic}}$$

where E_{Total} , E_{Thermal} , $E_{\text{Rotational}}$, $E_{\text{Vibrational}}$ and $E_{\text{Electronic}}$ are total energy, thermal energy, rotational energy, vibrational energy and electronic energy of tautomers, respectively. Total energy and Gibbs free energy include the zero-point energy and thermal corrections.

These parameters, which are E_{Total} and G° , were used to predict the stability. According to these parameters, ranking of tautomer stability should be as follow,

(1) > (2) \approx (3) (according to the E_{Total})

(1) > (3) \approx (2) (according to the G°)

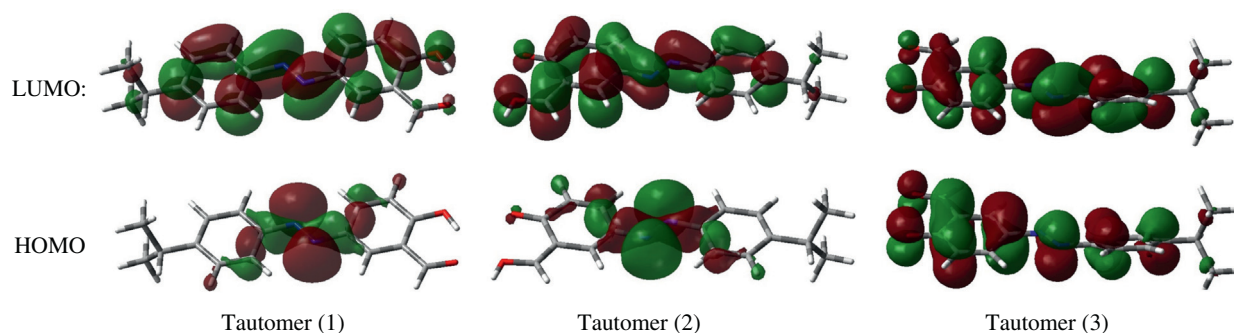


Fig. 9. Contour diagrams of frontier molecular orbitals for tautomers (1–3).

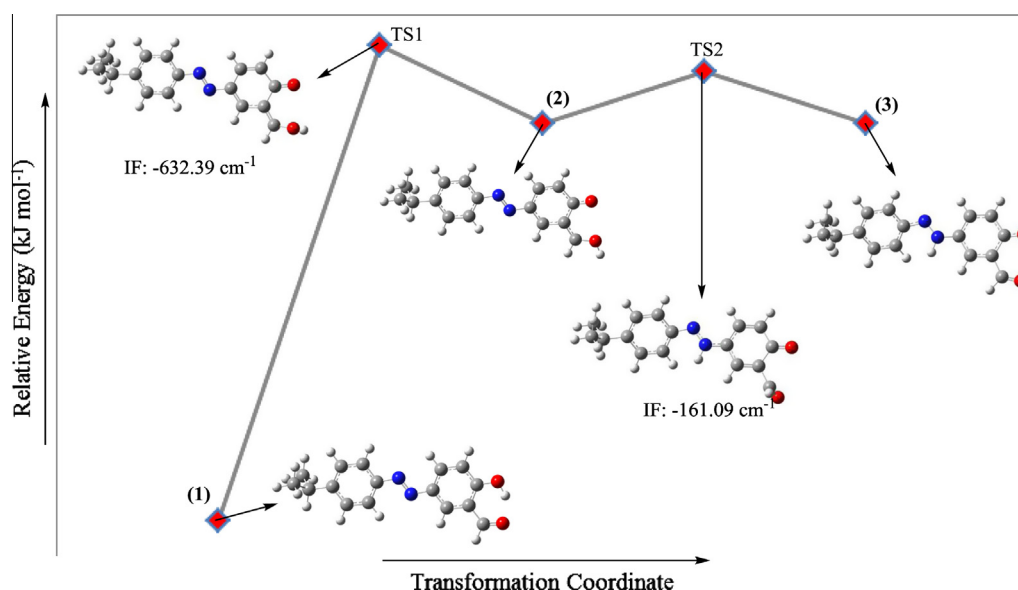


Fig. 10. The relative energy profile of tautomers (1–3), TS1 and TS2.

The tautomer with the lowest energy has the most stability. According to these rankings, the most stable tautomer is tautomer (1). The stabilities of tautomers (2) and (3) are close to each other.

Contour diagram of HOMO and LUMO can be used to predict the reactive region of tautomers. Contour diagrams of frontier molecular orbitals of tautomers were represented in Fig. 9.

HOMO is localized on (N=N) bond while LUMO is mainly delocalized on all atoms of molecules for tautomers (1) and (2). It can be said that the reactive regions of tautomers (1) and (2) are on N atoms. For tautomer (3), HOMO and LUMO are mainly delocalized on all atoms of molecule.

3.5. Transition states

The transformations between tautomers (1–3) were investigated by using transition state method. The transition states (TS) were calculated to explain the transformations. Imaginary frequencies (IF) indicate that the calculated structures are transition states. The total energies of tautomers (1–3), TS1 and TS2 were calculated. The total energy profile of them was represented in Fig. 10.

As can be seen from Fig. 10, tautomer (1) has the lowest energy. IF of TS1 and TS2 was found as -632.39 and -161.09 cm^{-1} , respectively. The conversion from tautomer 1 and 2, proton transfers from O1 to O2. For TS2, the structure rotates around C14–C16. There is a two proton transfer steps. The imaginary frequency of TS1 is higher than TS2. It indicates that TS1 is more near to reality

Table 4

Quantum chemical parameters of tautomers (1–3).

	Tautomer (1)	Tautomer (2)	Tautomer (3)
E_{Total} (kJ mol $^{-1}$)	-2308329.6	-2308212.0	-2308211.8
G° (kJ mol $^{-1}$)	-2308502.7	-2308387.8	-2308388.4

and conversion between tautomers 1 and 2 is more than conversion between tautomers 2 and 3.

3.6. UV-Vis. absorption spectra

The UV-Vis. absorption spectra of the azo aldehyde (ⁱpr-salH) and its Ni(II) chelate were investigated 200–800 nm range in different solvents (2×10^{-5} M CHCl_3 , MeOH and DMF). The absorption spectra of the compounds in different solvents are shown in Fig. 5S and the corresponding absorption wavelength maxima, absorbance and solvent properties (dielectric constant and dipole moment) are given in Table 5. The azo aldehyde (ⁱpr-salH) gave a maximum absorbance band ($\lambda_{1\text{max}}$) at 339 nm (CHCl_3), 349 nm (MeOH) and 408 nm (DMF). These absorption bands were assigned to $\pi \rightarrow \pi^*$ transitions of the aromatic rings. As the polarity of the solvent increases, maximum absorption wavelength shifted to longer values (bathochromic effect). In CHCl_3 and MeOH, there is also absorption as shoulder ($\lambda_{2\text{max}}$) at 419 and 421 nm, respectively, was assigned to $n \rightarrow \pi^*$ transition. In DMF which has higher

Table 5The UV–Vis. data of the azo-aldehyde and its Ni(II) chelate in various solvents (λ_{\max} , nm/cm⁻¹, absorbances, ϵ values).

Solvent	Dielectric constant	Dipole moment	Compound	$\lambda_{1\max}$ (nm/cm ⁻¹) (abs., $\epsilon \times 10^3$)	$\lambda_{2\max}$ (nm/cm ⁻¹) (abs., $\epsilon \times 10^3$)
CHCl ₃	4.8	1.04	ⁱ pr-salH	339/29,499 (0.241, 12.05)	431/23,202 (0.047, 2.35)
			[Ni(ⁱ pr-sal) ₂].5H ₂ O	349/23,202 (0.283, 14.15)	419/23,866 (0.098, 4.9)
MeOH	33	1.70	ⁱ pr-salH	350/28,571 (0.271, 13.55)	417/23,981 (0.092, 4.6)
			[Ni(ⁱ pr-sal) ₂].5H ₂ O	359/27,855 (0.291, 14.55)	421/23,753 (0.104, 5.2)
DMF	38	3.82	ⁱ pr-salH	408/24,510 (0.217, 10.85)	452/22,124 (0.238, 11.9)
			[Ni(ⁱ pr-sal) ₂].5H ₂ O	408/24,510 (0.276, 13.8)	446/22,422 (0.288, 14.40)

 λ_{\max} : Maximum absorption wavelength; abs.: maximum absorption intensity; ϵ : molar absorptivity coefficient (L mol⁻¹ cm⁻¹); sample concentration was 2.0×10^{-5} mol L⁻¹.

dielectric constants and dipole moment, the $n \rightarrow \pi^*$ transition was observed at 452 nm.

In the UV–Vis. absorption spectra of the complex [Ni(ⁱpr-sal)₂].5H₂O, maximum absorption wavelengths shifted to longer values (bathochromic effect) compared to the azo-aldehyde ligand indicating the complex formation. Absorption intensities also shifted to higher values compared to the ligand (hyperchromic effect). In all three solvents, the complex exhibits two absorption bands at 349, 419 nm (CHCl₃), 359, 421 nm (MeOH) and 408, 446 nm (DMF) were attributed to $\pi \rightarrow \pi^*$ ($\lambda_{1\max}$) and $n \rightarrow \pi^*$ ($\lambda_{2\max}$) transitions.

4. Conclusions

In conclusion, a novel azo-salicylaldehyde compound, 2-hydroxy-5-((*E*)-[4-(propan-2-yl)phenyl]diazonyl)benzaldehyde, ⁱpr-salH and its Ni(II) chelate were prepared and characterized by analytic and spectroscopic techniques. X-ray structure of the ligand indicated that there is a strong intramolecular hydrogen bonding (OH...O) in the structure. There is also inter-molecular phenol-aldehyde (OH...O) hydrogen bondings resulting a dimeric structure and stabilizing the structure. Optimized structures of the three possible tautomers of the ⁱpr-salH compound were obtained using B3LYP method with 6-311++G(d,p), 6-31G and 3-21G basis sets in the gas phase and B3LYP/6-311++G(d,p) level is found to be the best level for calculation. In the UV–Vis. absorption spectra of the complex [Ni(ⁱpr-sal)₂].5H₂O, maximum absorption wavelengths shifted to longer values (bathochromic effect) compared to the azo-aldehyde ligand indicating the complex formation.

Acknowledgements

The authors thank to Research Found of Kahramanmaraş Sutcu Imam University for financial support (Project No.: 2011/8-5 YLS). The authors are grateful to the Department of Chemistry, Loughborough University for providing X-ray laboratory for data collection.

Appendix A. Supplementary material

CCDC 947938 (ⁱpr-salH) contains the supplementary crystallographic data for this paper. These data can be obtained free of charge via www.ccdc.cam.ac.uk/data_request/cif, by e-mailing data_request@ccdc.cam.ac.uk, or by contacting The Cambridge Crystallographic Data Centre, 12 Union Road, Cambridge CB2 1EZ, UK. Fax: +44 (0)1223 336033. Supplementary data associated with this article can be found, in the online version, at <http://dx.doi.org/10.1016/j.molstruc.2014.02.052>.

References

- [1] A.J. Blake, N.R. Champness, P. Hubberstey, W.S. Li, M.A. Withersby, M. Schroder, *Coord. Chem. Rev.* 183 (1999) 17–138.
- [2] P.A. Vigato, S. Tamburini, *Coord. Chem. Rev.* 248 (2004) 1717–2128.
- [3] A.Y. Robin, K.M. Fromm, *Coord. Chem. Rev.* 250 (2006) 2127–2157.
- [4] S. Akine, T. Nabeshima, *Dalton Trans.* 47 (2009) 10395–10408.
- [5] X.F. Yang, P. Liu, L.P. Wang, M.L. Zhao, *J. Fluoresc.* 18 (2008) 453–459.
- [6] N. Narayanaswamy, T. Govindaraju, *Sensors Actuat. B* 161 (2012) 304–310.
- [7] J. Lu, H. Guo, X. Zeng, Y. Zhang, P. Zhao, J. Jiang, *J. Inorg. Biochem.* 112 (2012) 39–48.
- [8] M.T. Anitha, A.D. Naik, M. Nethaji, A.R. Chakravarty, *Inorg. Chim. Acta* 357 (2004) 2315–2323.
- [9] W.M. Cumming, G.J. Howie, *J. Chem. Soc.* (1933) 133–135.
- [10] P.J. Coelho, M. Cidália, R. Castro, A. Maurício, C. Fonseca, M. Manuela, M. Raposo, *Dyes Pigments* 92 (1) (2012) 745–748.
- [11] S. Sridev, S.U. Hiremath, C.V. Yelamaggad, S. Krishna Prasad, Y.G. Marinov, G.B. Hadjichristov, A.G. Petrov, *Mater. Chem. Phys.* 130 (2011) 1329–1335.
- [12] H. Zollinger, *Color Chemistry: Synthesis, Properties, and Application of Organic Dyes and Pigments*, Wiley-VCH, Weinheim, 2003.
- [13] R.N. Goyal, M.S. Verma, N.K. Singha, *Croat. Chem. Acta* 71 (3) (1998) 715–726.
- [14] P. Möller, H. Wallin, *Mut. Res.* 462 (2000) 13–30.
- [15] A. Kakanejadifard, F. Azarbani, A. Zabardasti, S. Kakanejadifard, M. Ghasemian, F. Esna-ashari, S. Omid, S. Shirali, M. Rafieefar, *Dyes Pigm.* 97 (2013) 215–221.
- [16] A. Halve, A. Goyal, *Orient. J. Chem.* 12 (2001) 87–88.
- [17] E.F. Lozinskaya, Y.M. Dedkov, *J. Anal. Chem.* 62 (2007) 788–793.
- [18] D.P.S. Rathore, M. Kumar, P.K. Bhargava, *Chem. Anal.* 40 (5) (1995) 805–813.
- [19] J. He, S. Bian, L. Li, J. Kumar, S. Tripathy, L. Samuelson, *J. Phys. Chem. B* 104 (2000) 10513–10521.
- [20] M.R. Yazdandbakhsh, M. Gahi, A. Mohammadi, *J. Mol. Struct.* 144 (2009) 145–148.
- [21] Bruker. APEX2 and SAINT Bruker AXS Inc., 1998.
- [22] G.M. Sheldrick, *Acta Cryst. A* 64 (2008) 112.
- [23] GaussView 5.0, Gaussian Inc., Wallingford, CT, USA, 2009.
- [24] Gaussian 09, AM64L-Revision-C.01, Gaussian Inc., Wallingford, CT, USA, 2010.
- [25] R.G. Parr, W. Yang, *Density-Functional Theory of Atoms and Molecules*, Oxford University Press, New York, 1989 (pp. 333).
- [26] N. Niazazari, A.L. Zatikyan, S.A. Markarian, *Spectrochim. Acta, Part A* 110 (2013) 217–225.
- [27] A.D. Becke, *J. Chem. Phys.* 98 (1993) 5648–5652.
- [28] C. Lee, W. Yang, R.G. Parr, *Phys. Rev. B* 37 (1988) 785–789.
- [29] P.J. Hay, W.R. Wadt, *J. Chem. Phys.* 82 (1985) 270–283.
- [30] J. Baker, *J. Comp. Chem.* 7 (1986) 385–389.
- [31] A.J.L. Jesus, L.N. Tomé, M. Ermelinda, S. Eusébio, M.T.S. Rosado, J.S. Redinha, *J. Phys. Chem. A* 111 (2007) 3432–3437.
- [32] M. Aslantas, N. Kurtoglu, E. Sahin, M. Kurtoglu, *Acta Cryst. E* 63 (8) (2007) O3637–U4709.
- [33] M. Odabaşoğlu, C. Albayrak, R. Özkanca, F.Z. Aykan, P. Lonecke, *J. Mol. Struct.* 840 (2007) 71–89.
- [34] H. Khanmohammadi, A. Abdollahi, *Dyes Pigm.* 94 (2012) 163–168.
- [35] H. Adams, D.E. Fenton, G. Minardi, E. Mura, A.M. Pistuddi, C. Solinas, *Inorg. Chem. Commun.* 3 (2000) 24–28.
- [36] (a) G.R. Desiraju, *Acc. Chem. Res.* 24 (1991) 290–296; (b) G.R. Desiraju, *Acc. Chem. Res.* 29 (1996) 441–449.
- [37] M. Bakir, G.R. Harewood, A. Holder, I. Hassan, T.P. Dasgupta, P. Maragh, M. Singh-Wilmot, *Acta Cryst. E* 61 (2005) o1611–o1613.
- [38] T.S. Basu Baul, S. Kundu, H.D. Arman, E.R.T. Tiekink, *Acta Cryst. E* 65 (2009) o3061.
- [39] O. Sahin, C. Albayrak, M. Odabasoglu, O. Buyukgungor, *Acta Cryst. E* 61 (2005) o4154–o4155.
- [40] O. Sahin, C. Albayrak, M. Odabasoglu, O. Buyukgungor, *Acta Cryst. E* 61 (2005) o4151–o4153.
- [41] O. Sahin, C. Albayrak, M. Odabasoglu, O. Buyukgungor, *Acta Cryst. E* 61 (2005) o4149–o4150.
- [42] C. Albayrak, M. Odabasoglu, O. Buyukgungor, P. Lonneck, *Acta Cryst. C* 60 (2004) o318–o320.
- [43] C. C. Ersanli, M. Odabasoglu, C. Albayrak, A. Erdonmez, *Acta Cryst. E* 60 (2004) o230–o231.
- [44] O. Sahin, C. Albayrak, M. Odabasoglu, O. Buyukgungor, *Acta Cryst. E* 61 (2005) o4276–o4278.
- [45] N. Karadayi, C. Albayrak, M. Odabasoglu, O. Buyukgungor, *Acta Cryst. E* 62 (2006) o1699–o1701.
- [46] O. Sahin, C. Albayrak, M. Odabasoglu, O. Buyukgungor, *Acta Cryst. E* 61 (2005) o4279–o4281.
- [47] N. Karadayi, C. Albayrak, M. Odabasoglu, O. Buyukgungor, *Acta Cryst. E* 62 (2006) o1727–o1729.
- [48] N. Karadayi, C. Albayrak, M. Odabasoglu, O. Buyukgungor, *Acta Cryst. E* 62 (2006) o3695–o3696.